COMPONENT PART NOTICE

THIS PAPER IS A COMPONENT PART OF THE FOLLOWING COMPILATION REPORT:

TITLE: Engine Response to Distorted Inflow Conditions: Conference Proceedings of the Propulsion and Energetics Specialists' Meeting (68th) Held in Munich, Germany on 8-9 September 1986.

TO ORDER THE COMPLETE COMPILATION REPORT, USE AD-A182 635.

THE COMPONENT PART IS PROVIDED HERE TO ALLOW USERS ACCESS TO INDIVIDUALLY AUTHORED SECTIONS OF PROCEEDING, ANNALS, SYMPOSIA, ETC. HOWEVER, THE COMPONENT SHOULD BE CONSIDERED WITHIN THE CONTEXT OF THE OVERALL COMPILATION REPORT AND NOT AS A STAND-ALONE TECHNICAL REPORT.

THE FOLLOWING COMPONENT PART NUMBERS COMPRISE THE COMPILATION REPORT:

AD#: P005 462 thru P005 473 AD#: _____

AD#: _____ AD#: _____

AD#: _____ AD#: _____

UNSTEADY INLET DISTORTION CHARACTERISTICS WITH THE B-1B

by

C. J. MacMiller
W. R. Haagenson
ROCKWELL INTERNATIONAL
NORTH AMERICAN AIRCRAFT OPERATIONS
P.O. Box 92098
Los Angeles, CA 90009
USA

SUMMARY

An extensive wind tunnel and flight test program has been conducted to verify inlet performance and distortion characteristics on the B-1B aircraft. During the course of these investigations, several unsteady, total-pressure disturbances at various discrete frequencies were encountered:

1) Inlet duct resonance at low power settings;
2) ECS precooler duct resonance; and
3) Nose gear wake ingestion.

This resulted in the need to quantify these effects and assess the impact on engine stability characteristics. As a result, engine control features were modified, and aircraft configuration changes were implemented. Results and findings of these investigations are summarized.

SYMBOLS

α	angle of attack
AIP	aerodynamic interface plane
B	superposition factor
β	sideslip angle
c	speed of sound
d	diameter
ψ	yaw angle
ECS	environmental control system
f	frequency
FAVG	engine face average total pressure (PT1)
FOD	foreign object damage
IDC	inlet distortion, circumferential
IDH	inlet distortion index, high-pressure (compressor) component
IDL	inlet distortion index, low-pressure (fan) component
IDP	index of planar distortion
IDPH	index of planar distortion, high-pressure (compressor) component
IDPL	index of planar distortion, low-pressure (fan) component
IDR	inlet distortion, radial
IGV	engine inlet guide vanes
IDTL	total distortion index, low-pressure (fan) component, combined spatial and planar distortion index
IDTH	total distortion index, high-pressure (compressor) component, combined spatial and planar distortion index
INT	intermediate power setting
K	1,000
KIAS	knots indicated airspeed
L	length
LG	landing gear
M	mach number
ΔP	pressure differential
P3G	planar pressure pulse generator
PK-PK	peak to peak
PLF	power for level flight
PSD	power spectral density
PT1	engine face average total pressure (FAVG)
PT0	freestream total pressure
RAVG	ring average total pressure
RCS	radar cross section
RMIN	ring minimum total pressure
RMS	root mean square
S	Strouhal number
T	temperature
W1R	engine corrected airflow
X	organ pipe end correction (sometimes set to 1.4d)
θ	sweep angle of ramp leading edge
Y_N	nacelle station, inches

INTRODUCTION

Stability characteristics of current high-performance turbofan engines are adversely affected by pressure fluctuations at the compressor face. One class of random pressure variations, frequently referred to as inlet-induced turbulence, is normally present in the flow. Engine stalls may result if sufficient energy/flow angularities exist at frequencies to which the compression system may respond. Dynamic distortion factors are used to correlate these types of pressure variations with losses in engine surge margin. Critical events can be difficult to define and usually require stochastic techniques. Correlations between the resulting spatial distortion characteristics and loss in surge margin have been the subject of considerable resources during recent decades (References 1 and 2).

Another class of pressure fluctuations can be destabilizing and is attributed to the occurrence of one-dimensional, unsteady-pressure oscillations at the compressor face. Inlet buzz during supersonic operation at low inlet mass flow ratios is one classic example of a large-amplitude, planar wave coupled with spatial distortion. These transients are generally characterized by discrete frequency components and thus classified deterministic. Although higher frequency components are present, events are readily identified.

Reported sources of planar pressure oscillations include both internally and externally generated disturbances. Internally-generated disturbances include flow separation/reattachment, turbulence, buzz, unstart/restart cycles, interaction with adjacent engines and inlets, response to control system inputs and secondary air inlet designs. Examples of externally generated disturbances include armament firing, atmospheric gusts, wakes of previous aircraft, external explosions and ingestion of wakes emanating from forward protuberances - landing gear, external stores and pylons, aerodynamic surfaces, and weapon bay doors and spoilers. Methods for dealing with the simultaneous effects of planar and spatial total-pressure fluctuations are not well understood.

An extensive wind tunnel program was conducted to develop the B-1B propulsion system, and a flight test program to verify operational suitability is well underway. During the course of the investigations, numerous instances were encountered where discrete frequency components were evident in total pressures at the engine inlet. This resulted in the need to quantify the effects and assess impact on engine stability characteristics. As a result, engine control features were modified, and aircraft configuration changes were implemented. Results and findings of these investigations, including wind tunnel and flight test comparisons, are summarized.

B-1B PROPULSION SYSTEM

The B-1, Figure 1, is a long-range strategic aircraft operated by a crew of four. Distinctive features relative to the propulsion system are variable sweep wings, nose gear protuberances forward of the inlets, external stores, structural mode control vanes and weapon bay doors and spoilers. The variable wing changes the wing sweep angle from 15 to 67.5 degrees. The aft sweep position (67.5 degrees) is used at high speeds and during low altitude penetration. The structural mode control vanes are located on the lower sides of the forward fuselage and vary to control structural bending mode oscillations and to provide a smoother ride quality.

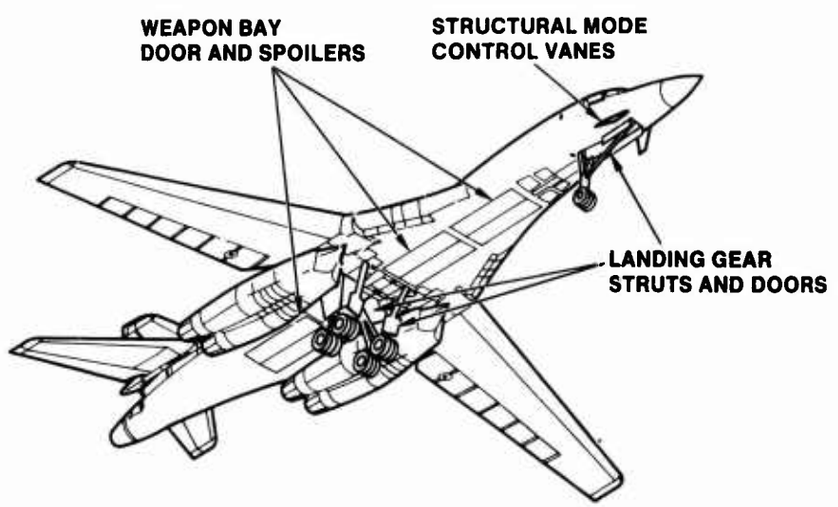

Figure 1. B-1B Air Vehicle

The B-1 propulsion system consists of two nacelles mounted under the fixed portion of the wing. Each nacelle contains two General Electric afterburning turbofan engines, and separate, independent inlets and

diffusers. Inlets are two-dimensional, with vertical compression ramps, and are located aft of the wing glove leading edge, outboard of the aircraft centerline. Forebody/wing boundary layer air is removed by a gutter located between the nacelle and wing. The off-centerline location required a complete flow field investigation because of wing flow outwash that varied with angle of attack, particularly at the aft wing sweep position. Nacelles are toed-in 1/2 degree to align with local flow at nominal angles of attack.

The B-1B inlet nacelle is a modification of the B-1A nacelle and not a complete redesign. A drawing of the B-1B inlet, illustrating some of its unique features, is shown in Figure 2. External nacelle mold lines were unchanged from the B-1A so as to not impact structural attachments and/or landing gear and nacelle clearances. Internal mold lines were modified with gradual bends and vanes to improve RCS characteristics. The region in the center of the nacelle, which housed the variable ramps and actuators of the B-1A, provided the space for the bends and vanes. Leading edges of cowls and vanes were canted 15 degrees to further enhance RCS characteristics. The center ramp was cut back 41 degrees to reduce planar pulse amplitudes and to reduce RCS. A three-position, movable cowl lip is employed to improve takeoff and low-speed performance and distortion. ECS scoops, internal to the inlet, precool engine bleed air above mach 0.5. This air exhausts between engine nozzles at the rear of the nacelle. At speeds below mach 0.5, precooler air is provided through separate inlets located outside the nacelle, above the wing, operating in conjunction with a blower. Flapper valves are used to prevent blower air from entering the main inlets.

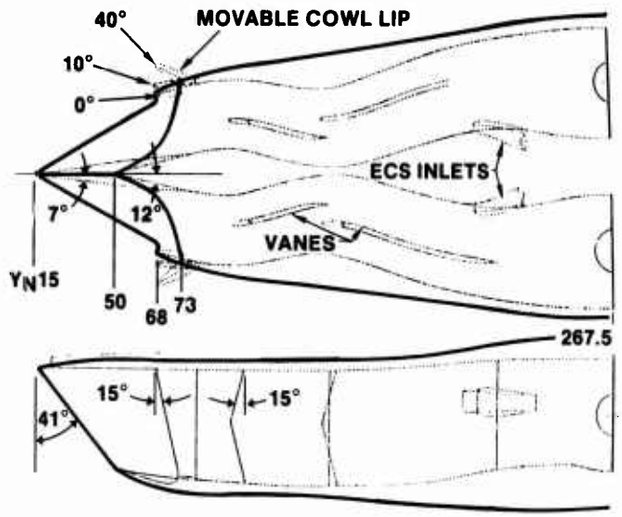

Figure 2. B-1B Inlet Nacelle

AERODYNAMIC INTERFACE PLANE INSTRUMENTATION

The inlet/engine aerodynamic interface plane (AIP) is the instrumentation station used to define total-pressure recovery and distortion interfaces between the inlet and the engine. In the B-1 program, the interface was defined at the leading edge of the engine inlet guide vanes (IGV). All airflow passing through this plane enters the engine. This instrumentation station was used throughout the inlet development and verification wind tunnel program, during engine qualification tests, and is being used in the ongoing flight test program.

Eight rakes, each with five probes located at the centroid of equal annular areas, were used to measure pressures. Small differences in angular location were necessary among models due to the evolving nature and availability of particular IGV locations. All probes in the resulting 40-probe matrix were designed to measure both the steady-state and high-response components of total pressure. Leading edges of probes were chamfered to minimize sensitivity to flow direction. Distortion components, both radial and circumferential, were computed for each of five rings from eight total-pressure measurements on each ring.

A photograph of the AIP instrumentation used during 0.2-scale wind tunnel testing is shown in Figure 3. To maintain required frequency response, miniature high-response transducers were physically located at the AIP. Signals were high-pass filtered (A.C. coupled) to maintain accuracy over a wide range of pressure levels. These same dual-purpose probes provided a sensed location for the low-response (steady state) pressure measurements with larger, more accurate transducers. These transducers were located remotely in an environmentally-controlled area. A flow-control valve was located as close as possible to the AIP. During most tunnel operating conditions, airflow through this valve was choked, providing a reflection plane to simulate inlet acoustic properties.

Flight test AIP instrumentation is also shown in Figure 3. High-response transducers were installed integrally with selected IGV's. With appropriate signal conditioning, measurements of steady-state and

high-response outputs were recorded separately from the same transducer. An inflight calibration system was used to automatically provide a zero and a one-point pressure calibration throughout the flight at one-minute intervals. Generally, experience has shown good agreement between wind tunnel and flight test results (Reference 3). The relatively small differences in AIP instrumentation matrices and signal conditioning systems between wind tunnel and flight test produced only second-order effects on measured inlet distortion characteristics.

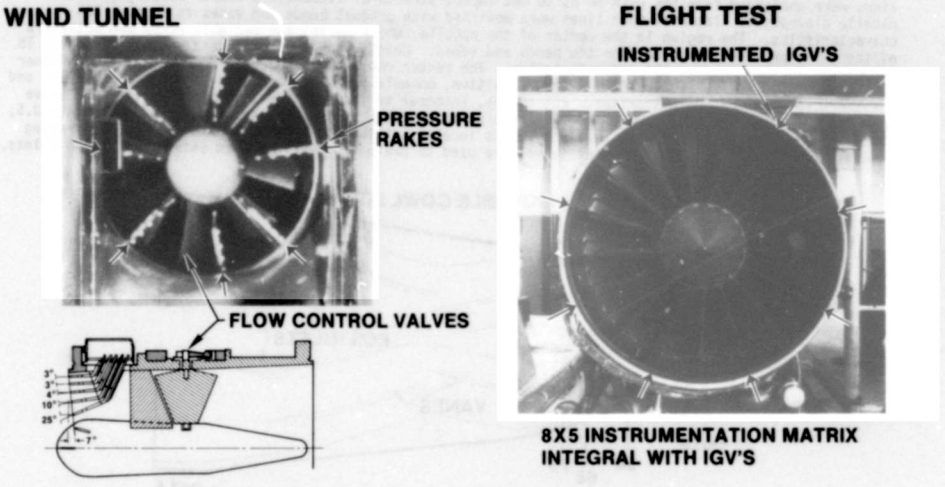

Figure 3. Aerodynamic Interface Plane Instrumentation

DISTORTION ASSESSMENT PROCEDURES

Distortion methodology is defined as the set of procedures used to specify numerical values of spatial and planar total-pressure components at the selected measurement plane. Distortion descriptors are calculated from the spatial and time-dependent distribution of total pressures at the aerodynamic interface plane and are based on measurements from the 40 total-pressure probes defined in the previous section. They are used to define inlet spatial distortion characteristics with a time duration of sufficient length to affect engine stability. Additionally, they are used to describe amplitudes and frequency variations in the spatially-averaged pressure time histories, sometimes referred to as planar distortion. Variations occurring at discrete frequencies are "book-kept" as planar distortion and may also contribute to engine instabilities. Accurate measurement of these frequency components depends on the simulated engine face acting as an acoustic reflection plane.

Spatial distortion factors were generated in accordance with the procedures defined in Reference 1. With the 8 x 5 instrumentation array, circumferential and radial distortion components for each of the five rings are computed according to the following relationships:

CIRCUMFERENTIAL

$$IDC = \frac{RAVG-RMIN}{FAVG}$$

RADIAL

$$IDR = \frac{FAVG-RAVG}{FAVG}$$

Ring components can be combined in various ways to define overall engine face descriptors. Radial distortion components located in the outer diameters are frequently referred to as "tip radials", radial components located in the inner diameter are referred to as "hub radials". Distortion components are computed from high-response total-pressure signals filtered to the critical engine frequency and digitally sampled at rates sufficiently high to retain wave form. Resulting envelopes, encompassing all combinations of circumferential and radial distortion components, are used to describe distortion characteristics for a particular operating condition and/or inlet geometry and are illustrated in Figure 4. By imposing estimated engine limits on this same grid, a particular distortion pattern can be identified that consumes more stall margin than any other point and can be used to characterize spatial distortion for that particular data point. Estimated engine limits for a particular operating condition can also be used to normalize measured distortion levels and thus provide convenient indices, IDL and IDH, whose values are unity when measured distortion equals engine distortion allocations. These procedures can be applied separately to both the fan and compressor to gain insight on the controlling engine module.

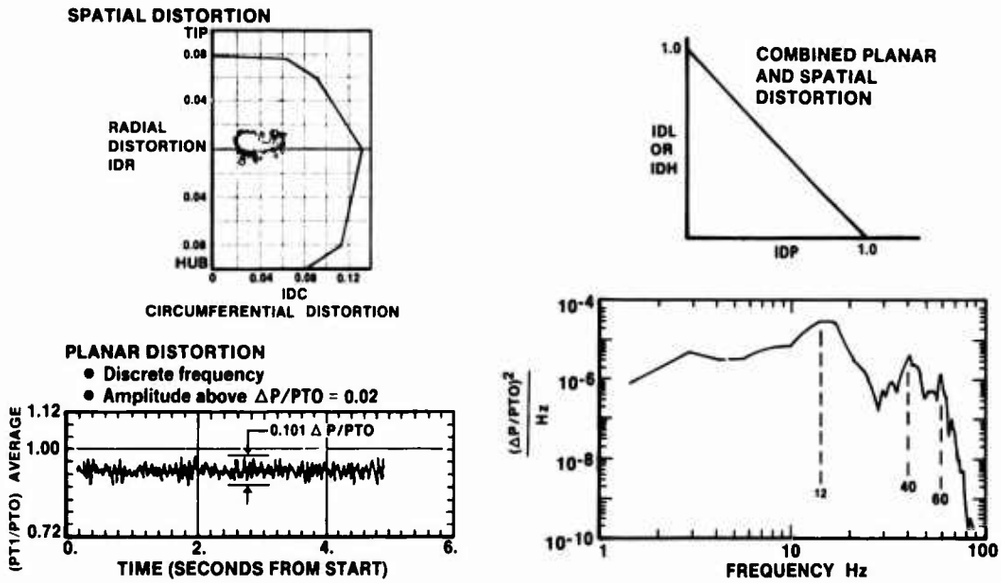

Figure 4. Distortion Assessment Procedures

Planar distortion components on the B-1B were measured during wind tunnel tests by routing all 40 high-response AIP signals to a summing circuit and outputting the numerical average. Power spectral densities (PSD) of the resulting analog signal were used to identify the presence of discrete frequency components and the magnitude of the energy contained within each frequency band. Initial estimates on sensitivity to planar distortion were based on extrapolations from F101 fan/P3G testing completed in 1973 (Reference 4). A PSD of a signal containing multifrequency planar distortion components is illustrated in Figure 4. An index of planar distortion (IDP) is generated by normalizing measured energy to estimated limits. When more than one discrete frequency component exists, individual contributions are summed linearly to obtain the total index.

Above assessments of planar distortion are based on two assumptions. One, that planar distortion is transferred without diminishment by the fan; and two, the fan and compressor planar distortion sensitivities are similar. Data supporting these assumptions are sparse, but it is logical to expect that at high levels of IDP, at some frequencies, fan or compressor instabilities can result even in the absence of spatial distortion. When planar distortion is imposed on spatial distortion, it follows that allowable spatial distortion is therefore decreased. Again, data supporting this premise are essentially nonexistent.

Screening procedures used on B-1B wind tunnel and flight test data assume that spatial and planar distortion indexes add linearly (B = 1.0) to provide a combined measure of inlet distortion.

FAN	COMPRESSOR
IDTL = IDL + B (IDPL)	IDTH = IDH + B (IDPH)

In subsequent sections, these indexes are used as an initial step in assessing B-1B inlet/engine compatibility. They provide useful tools to screen a large number of data points to identify potential areas of concern and to quantify incremental differences among a host of configuration and operating variables. Distortion characteristics that survive initial screening procedures are subject to more detailed analysis. These may include transient runs with engine dynamic simulations, stability stack-ups more tailored to the particular configuration and operating procedures, and statistical assessment procedures to put potential problems in perspective and suggest design alternatives.

INTERNALLY-GENERATED DISTURBANCES

Two sources of inlet-generated disturbances encountered during the development of the B-1B propulsion system are discussed. In one case, local flow separation occurred along the external inlet ramp surface and resulted in duct resonance during low-power engine operation at leeward sideslip. In another case, an ECS scoop, located within the inlet to precool engine bleed air, resonated under "no flow" conditions, and resulting disturbances were recorded with high-response, total-pressure instrumentation located at the aerodynamic interface plane. Both instances were characterized by a coupling between discrete frequency

components and spatial distortion components normally present in the flow. Although engine response to this coupling is not well understood, a need to evaluate inlet-to-engine compatibility in the presence of combined planar and spatial distortion was clearly identified.

INLET DUCT RESONANCE

Low-airflow planar distortion is caused by local flow separation and reattachment along the ramp surface forward of the cowl during leeward sideslip as shown in Figure 5. Separation and reattachment cycles occur at the 11 Hertz closed-end organ pipe frequency of the inlet duct measured to the acoustic interface of the engine. Circular flow patterns shown on the sketch were evident from oil-dot flow patterns measured in wind tunnel tests.

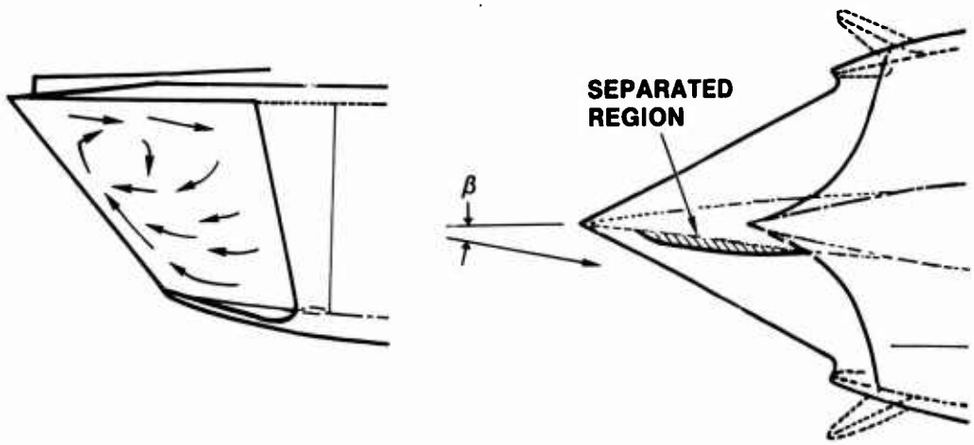

Figure 5. Local Flow Separation on Inlet Ramp During Off-Design Operation at Low-Airflow

Local ramp separation at low airflows and leeward sideslip is due to a highly adverse pressure gradient forward of the cowl lip station interacting with boundary layer along the forward ramp surface. As leeward sideslip increases, the flow expands around the ramp leading edge, then decelerates rapidly to the inlet station. Local ramp pressures decrease near the leading edge which allow boundary layer thickness to increase prior to entering the high-pressure-gradient region. The process is similar, although at much lower amplitudes, to buzz at supersonic speeds caused by shock wave and boundary layer interactions. Horizontal ramp inlets experience this phenomena at low or negative angles of attack; vertical ramp inlets at leeward sideslip.

Representative distortion characteristics recorded during wind tunnel tests at mach 0.85 with the outboard inlet are shown in Figure 6. The model was positioned at nine-degrees angle of attack and five degrees sideslip. Flow field measurements identified that local outwash, generated by the fuselage and wing combination, increases proportionately with angle of attack. Angle of attack and sideslip thus act in concert to orient the outboard ramp leeward and produce the distortion characteristics shown as a function of engine corrected airflow.

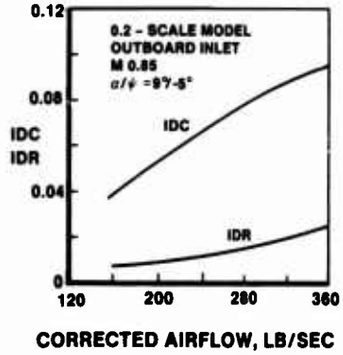

Figure 6. Spatial Distortion Characteristics

Circumferential distortion is the predominant spatial component, although both components increase almost proportionately with corrected airflow. Flight test results generally confirm wind tunnel results. Time histories of the average of the 40 individual AIP signals indicate that in addition to these spatial distortion components, the flow, at this off-design condition, is experiencing a one-dimensional oscillation about a mean, and peak-to-peak amplitudes of this combined signal can be used as a figure of merit. One example at low corrected airflow is shown in Figure 7. Power spectral densities identify the presence of discrete frequency components with a fundamental frequency of 60 Hertz (0.2-scale). This frequency corresponds well with organ pipe theory, $f = c/[4(L + X)]$, where the characteristic dimension is controlled by the distance between the average cowl leading edge and the AIP. The presence of odd-numbered harmonics is consistent with closed-end organ pipe theory.

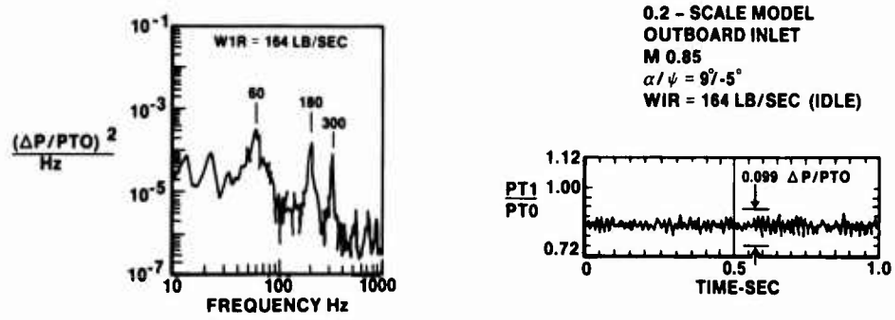

Figure 7. Planar Distortion Characteristics

Magnitudes of these planar waves are strong functions of several independent parameters - geometry, corrected airflow, attitude and mach number. The ramp serves as a separation plane to maintain inlet-to-inlet independence. However, tests were conducted to measure the effectiveness of increasing the sweep angle of the ramp leading edge in an attempt to eliminate, or at least minimize, the source of the flow separation. This proved to be an effective technique to reduce the magnitude of the planar wave. Variations of peak-to-peak amplitude for two leading edge sweep angles are shown as a function of corrected flow in Figure 8. During off-design operation at mach 0.85, at airflows corresponding to operation at IDLE power, increasing the sweep angle from zero to 41 degrees reduced the amplitude of the planar wave by almost 50 percent. No evidence of disturbances at the AIP in the adjacent inlet was detected. Subsequent testing at other mach numbers and maneuver conditions verified that inlet-to-inlet independence could be maintained with the cut-back ramp.

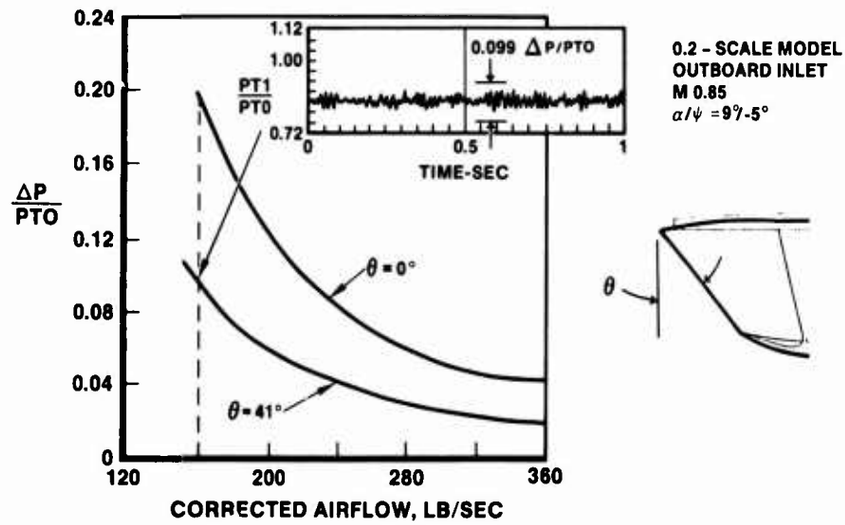

Figure 8. Effect of Ramp Leading Edge Sweep on Planar Wave Amplitude

Tests showed that the magnitude of the planar wave was sensitive to mach number, airflow and attitude as illustrated for the outboard inlet in Figure 9. At normal cruise attitudes, where the degree of outwash is small, planar amplitudes remain below two percent throughout the mach range. As local outwash is increased, by operation at combinations of angles of attack and sideslip, sensitivities to mach number increase markedly, and at sonic conditions, amplitudes can approach 12 to 15 percent of freestream total pressure. At high subsonic mach numbers, amplitudes of these planar waves can be reduced by almost 50 percent by increasing flight idle airflows to rates corresponding to 90 percent core corrected speed. This feature is sometimes referred to as "idle-speed lockup".

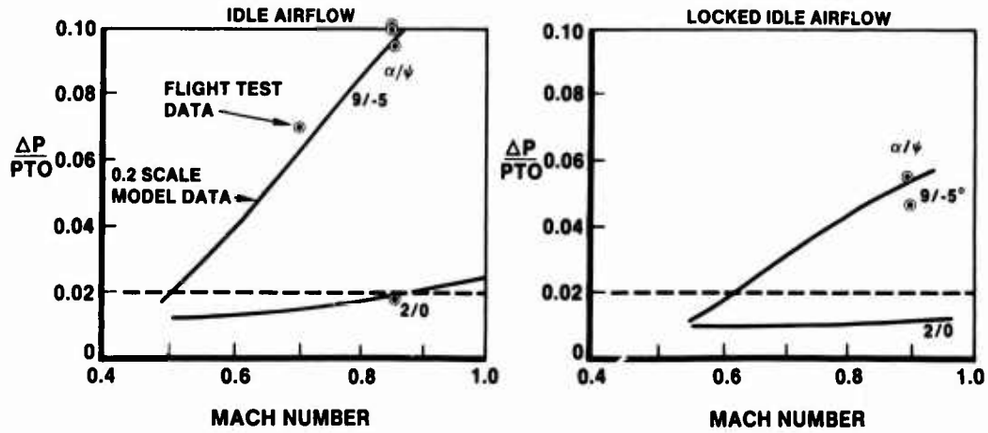

Figure 9. Planar Wave Amplitude Characteristics With Outboard Inlet

Good agreement in both magnitude and frequency of planar distortion were obtained between wind tunnel and flight test results. One example is shown in Figure 10, comparing time histories of comparable signals during leeward operation at mach 0.85 and airflows corresponding to IDLE power. Peak-to-peak amplitudes of ten percent were measured directly with both the airplane and the 0.2-scale wind tunnel model. And frequencies scaled directly with Strouhal number, $S = fL/\sqrt{T}$, resulting in a full-scale frequency of 12 Hertz, well within the frequency range to which engines respond.

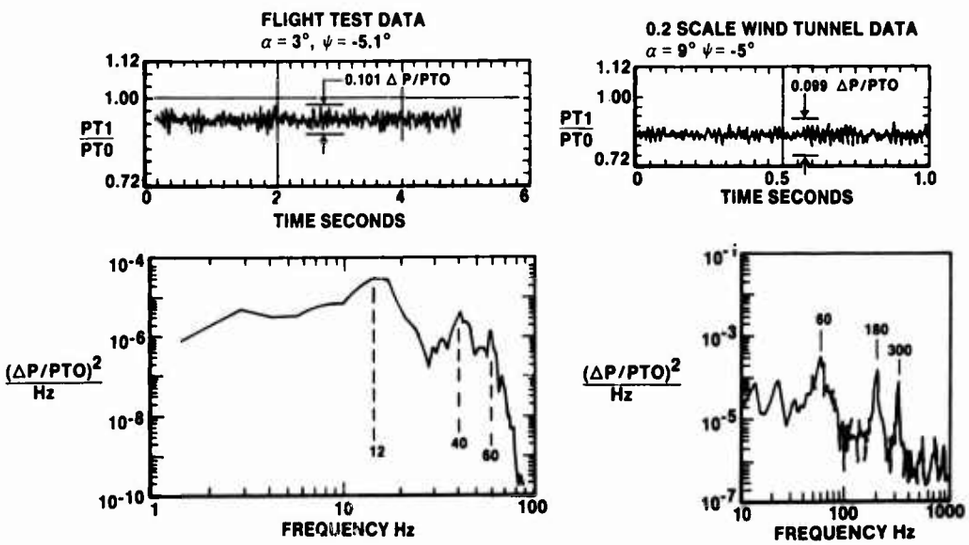

Figure 10. Wind Tunnel/Flight Test Comparison of Planar Distortion, Mach 0.85, Outboard Inlet, W1R = 164 lb/sec

Ramp separation and the associated planar distortion component are thus shown to be fundamentally a low-airflow phenomenon. Fortunately, spatial distortion components are directly proportional to airflow and are typically less than four percent at idle airflow. At first glance, one would expect this to be compensatory; however, engine tolerance to spatial distortion can be strong functions of engine corrected airflow and compression system rotational speeds. In fact, the need to accelerate the engine during periods of thermal mismatches between the engine case and rotor, as, for example, during a throttle bodie, can be one of the more difficult hurdles for inlet/engine stability assessments. Complexities of assessing the impact of adding a planar distortion component make it that much harder.

Using a simplifying assumption that superposition factors defining the relationship between planar and spatial distortion components are unity, assessments were conducted over a range of airflows, mach numbers, and angles of attack and sideslip using data recorded during wind tunnel tests with the 0.2-scale inlet verification model. Because engine sensitivity is also a function of altitude, conditions were evaluated at altitude extremes for each mach number, and for both fan and compressor engine modules.

Typical results are illustrated in Figure 11 during operation at mach 0.85. Maneuver conditions are identified where engine stability margin allocations to the inlet are fully utilized. In an adverse combination of events, where throttle transients are performed on deteriorated engines with worst case engine control tolerances, occasional engine stalls would be anticipated during operation outside the maneuver envelopes shown. In most cases, stability limits for the compressor are reached before margin runs out on the fan. Limiting maneuver conditions at negative yaw (positive sideslip) represent limitations of the No. 1 inlet (left-hand, outboard). Mirror images of these limitations, shown at positive yaw (negative sideslip) represent operation of the No. 4 inlet (right-hand, outboard). Occasional instabilities would be predicted for both outboard inlets during operation at angles of attack above the intersection of these lines.

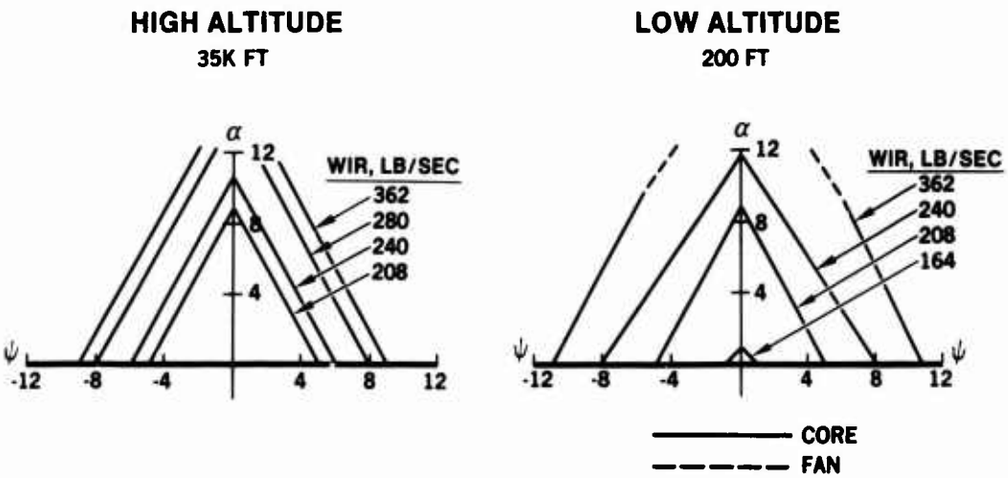

Figure 11. Stability Assessment During Mach 0.85 Maneuvers

Historically, one objective of good inlet/engine design is to maintain stall-free engine operation under fleet conditions throughout the anticipated flight and maneuver envelopes. To achieve this objective with the B-1B/F101, the foregoing methodology and analyses indicate that within portions of the flight envelope, engine corrected airflow should be maintained above 210 lb/sec. Consequently, an idle speed lock-up feature was incorporated and is implemented by a manual switch located in the crew station. When activated, one switch controls all four engines and limits core operation to 90 percent corrected speed. Thrust modulation with this setting is adequate to meet all aircraft requirements in all atmospheres. Temporary handbook instructions currently require activation of this mode of operation above 425 KIAS or mach 0.9, whichever is less. Ongoing flight test evaluations of this system will help to determine the need, and if need be, suggest potential means of automating implementation.

AUXILIARY AIR INLET

Auxiliary air inlets can be another source of internally generated disturbances. A scoop is installed on the ramp side of each B-1B inlet to precool ECS bleed air. During ground and low speed operation, when inlet pressure is lower than ambient, a hydraulically-driven blower supplies outside air to the heat exchanger. A flapper door, installed in the common duct connecting these sources of cooling air, is closed to prevent reverse flow during blower operation. Air is exhausted aft through exits located between engine nozzles to reduce base drag. At mach 0.5, pressure in the inlet duct is sufficiently above ambient pressure to service the heat exchanger. The blower is shut off and the flapper door opens allowing air to flow through the scoop inlet.

The design and relative location of the ECS precooler inlet assembly is shown in Figure 12. The scoop is located just above the duct centerline and extends four inches into the inlet. The scoop had to be redesigned to accommodate the redesign of the basic B-1B inlet. Advantage was taken of this opportunity to reshape the scoop cowl lip and external mold line to minimize external flow separation under "no flow" conditions. The scoop thus acts as a resonator (closed organ pipe) with the controlling volume located between the leading edge and the flapper valve. Since the flapper door is self-positioned by air loads, resonance can lead to structural damage, particularly during operation close to the transition point when the pressure differential across the door is small. Because of the low duct pressure, engine FOD can result, and during the initial B-1B flight test program, several instances were attributed to structural failure within this system.

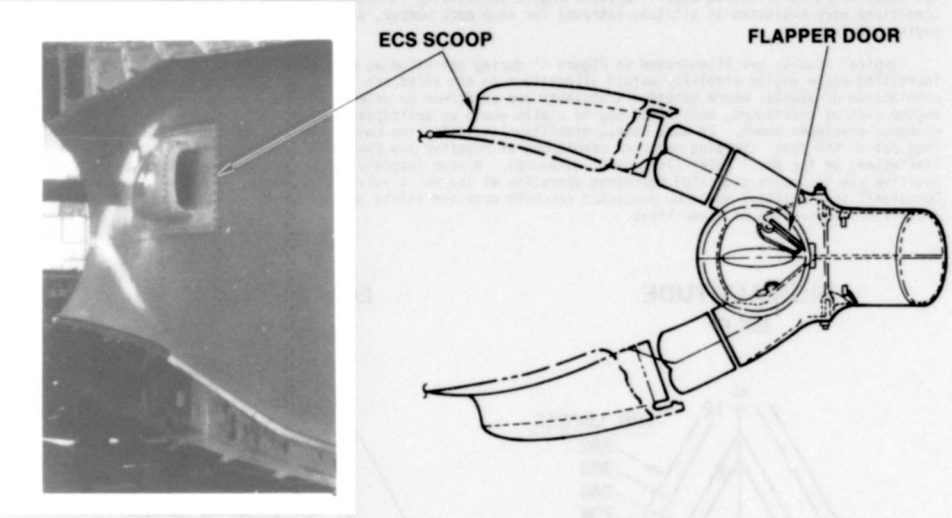

Figure 12. ECS Precooler Assembly

High-response pressure transducers located just upstream of the flapper door in the aircraft identified duct resonance at frequencies corresponding to a closed-end organ pipe. During static operation on the ground at maximum engine airflow, power spectral densities, Figure 13, identified a fundamental frequency at 77 Hertz as well as the presence of several harmonics. RMS amplitudes were approximately 2.4 psi. Similar results were obtained with the 0.2-scale inlet model. Although amplitudes were smaller, discrete components were measured at scaled frequencies, and a program was initiated to eliminate and/or reduce the magnitude of these oscillations.

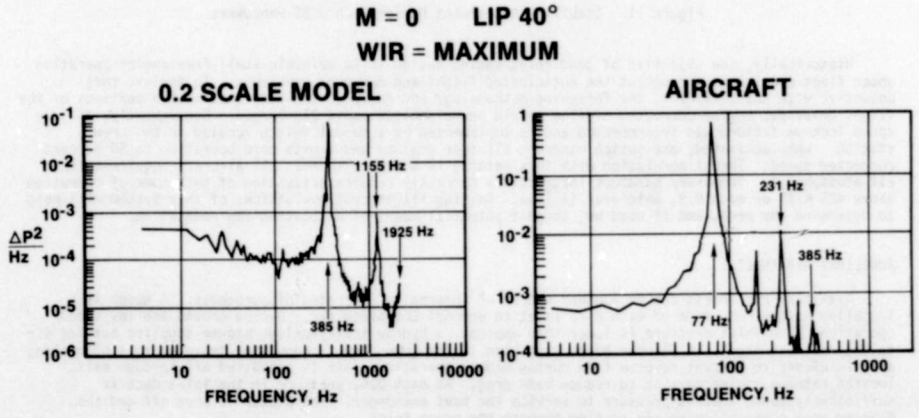

Figure 13. Resonance Characteristics in ECS Scoop Inlet

Two areas of concern were addressed. One was to explore potential configuration changes to eliminate the disturbance, and the other was to ensure that changes had no adverse impact on engine stability. Wind tunnel results showed that disturbances propagated both upstream and downstream in the duct as shown in Figure 14. Spatial measurements at the aerodynamic interface plane showed that a majority of the probes registered discrete frequency components, and could thus induce planar distortion components. Probes located on the same side as the ECS scoop contained more energy at discrete frequencies. While frequencies were generally beyond the engine 62.5 Hertz cut-off frequency corresponding to "one per rev" (300 Hertz at 0.2 scale), configuration changes could alter downstream frequency components, impact spatial distortion characteristics, and affect engine stability.

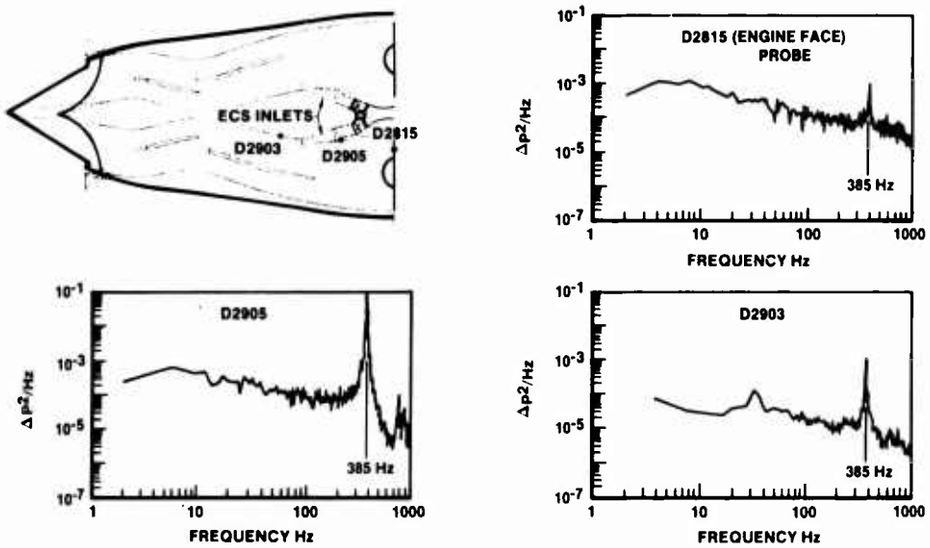

Figure 14. Acoustic Resonance Propagation From ECS Scoop Inlet

Tests were conducted in a Rockwell static facility with the 0.2-scale inlet model. Several concepts were investigated to reduce or eliminate duct resonance. One concept consisted of changing the valve design to "leak" reverse flow back through the scoop. By restricting the leakage flow rate, penalties on heat exchanger performance could be minimized. Another concept consisted of a bypass arrangement designed to provide continuous airflow through the scoop to reduce acoustic amplitudes. Yet another concept consisted of designing a resonator chamber upstream of the valve to attenuate specific frequencies.

Test results with the reverse-flow concept are shown in Figure 15. Power spectral densities generated from a high-response, static-pressure transducer located close to the valve are shown for three valve positions. Although discrete-frequency components are evident for all valve settings, total energy under the curve - a measure of peak-to-peak amplitude - decreases rapidly with increased flow area. With an area equivalent to 2.0 square inches full scale, total energy is reduced by approximately two orders of magnitude. Similar results were obtained with the bypass and resonator configurations. As a result of this experience, subsequently confirmed with full-scale tests, the B-1B production redesign incorporates a snubber and a leakage area of two square inches. No problems have been encountered upon incorporation of these changes.

EXTERNALLY-GENERATED DISTURBANCES

Several sources of externally generated disturbances were also encountered during the development of the B-1B. Generally, these disturbances can be traced to wakes and vortices shed from external surfaces. It is not unusual for these disturbances to contain discrete-frequency components. For example, structural mode control (SMC) vanes are located on the lower forward fuselage. Sinusoidal deflections of these vanes are designed to attenuate relative structural motion between the crew station and the aircraft center of gravity and thus provide good ride qualities. Under certain maneuver conditions, vortices generated by these surfaces can be ingested by the inlet. During the B-1A program, a considerable effort, including full-scale inlet/engine tests, was conducted to verify airframe/engine compatibility during operation of this system, and results are well documented in Reference 5.

Nose gear wake ingestion is another source of externally generated disturbances. Flight test investigations with the B-1 configurations have shown that nose gear wakes do contain discrete frequency components, identifying another need to assess engine stability characteristics with combined planar and spatial distortion components. Based on assessments derived from extensive wind tunnel tests and limited engine response characteristics, a movable cowl lip was incorporated in the B-1 inlet design. Cowl lip

angle is held in one of three positions, 40, 10 or 0 degrees, and is scheduled as a function of gear position and mach number as shown in Figure 16. Good performance and acceptable distortion characteristics during takeoff and low-speed operation result, and drag is minimized during high-speed flight.

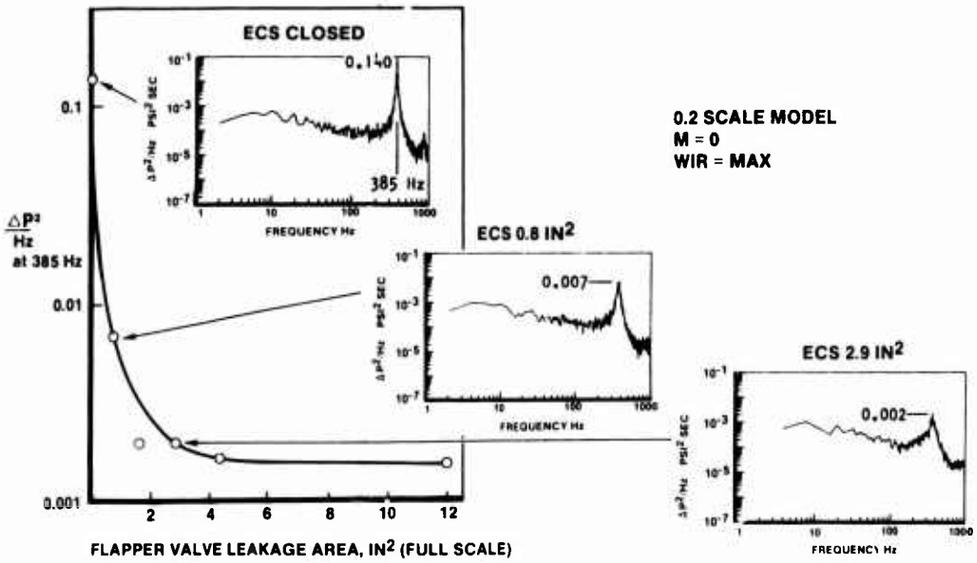

Figure 15. Effect of Reverse Flow on Acoustic Amplitude in ECS Scoop

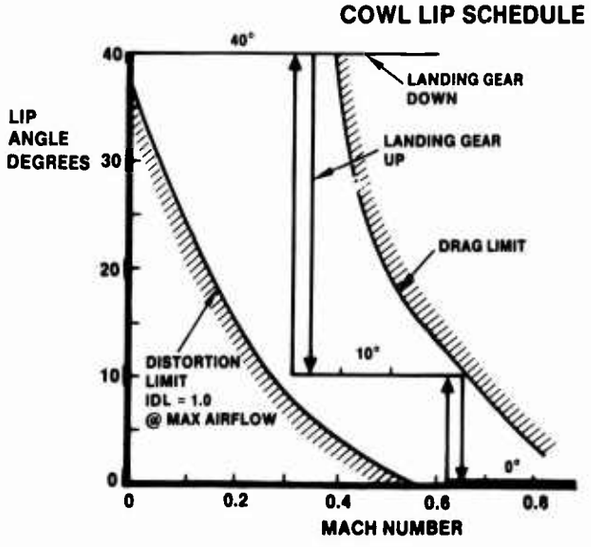

SWITCHING LOGIC	
SWITCHING	COMMAND
40° → 10°	M 0.35 INCR AND LG UP
40° ← 10°	M 0.32 DECR OR LG DOWN
10° → 0	M 0.65 INCR
10° ← 0	M 0.62 DECR

Figure 16. Cowl Lip Schedule

Limits that define regions of acceptable lip operation are also shown. The distortion limit was derived from wind tunnel data and defines regions where combined spatial and planar distortion levels remain within engine allocations. The limit shown for drag is somewhat arbitrary. Drag increases with increasing lip angle and/or mach number and eventually becomes excessive. Operation at mach numbers and lip angle combinations greater than this limit are avoided to minimize impact on specific fuel consumption during important mission conditions.

Switching among the 40-, 10-, and 0-degree cowl lip settings is based on flight mach number and landing gear position. The 40-degree lip setting is used for takeoff and all flight conditions where the landing gear is down and the nose gear wake could enter the inlet. The 10-degree lip position is used above mach 0.35 after the landing gear is raised. This position maintains inlet distortion levels within engine allocations for flight maneuvers up to mach 0.65. The fully closed, 0-degree position is used for high-speed operation above mach 0.65 where drag is critical. The cowl lip reopens as flight speed is reduced and/or the landing gear is lowered. An increment of 0.03 in mach number is used to separate opening and closing signals to provide a positive control input in both directions.

Circumferential distortion characteristics derived from high-response AIP signals during wind tunnel tests are shown in Figure 17 as a function of mach number and cowl lip angle at maximum engine corrected airflow. Both parameters have a profound impact on spatial distortion levels, and this is attributed to local flow separation on the cutback cowl lip. Large expansion turning angles between the stagnation streamline and local cowl mold line occur in this region at high inlet mass flow ratios. Levels are aggravated by sideslip in the direction making the inlet windward; i.e., nose left sideslip for inlets 2 and 4, and nose right sideslip for inlets 1 and 3. Spatial distortion levels measured during flight tests agree well with wind tunnel results as shown for selected configurations and mach numbers.

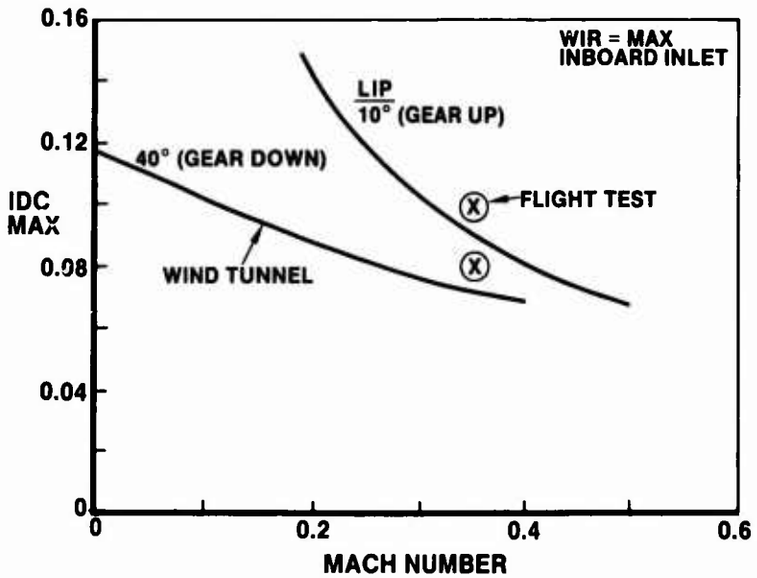

Figure 17. Effect of Cowl Lip Position on Spatial Distortion

With the gear extended, planar distortion components were also evident in the flow. Variations in peak-to-peak amplitudes of the average engine face total pressure are shown in Figure 18 as a function of freestream mach number. The amplitude is independent of lip position and is essentially eliminated by retracting the gear. Peak-to-peak amplitudes of approximately five percent were measured in the wind tunnel at mach 0.35. Amplitudes recorded during flight tests at comparable conditions approached seven percent. Differences are attributed to atmospheric uncertainties during flight test and to problems encountered in accurately simulating complex landing gear structure in small scale models. Discrete frequency components were evident in power spectral densities generated with these signals at all airflows. With flight test data, the fundamental frequency was 18 Hertz at mach 0.4, increasing to 28 Hertz at mach 0.6.

Sideslip transients with the gear extended were conducted during flight at mach 0.4 at an altitude of 10,000 feet. Resulting spatial and planar distortion characteristics are shown in Figure 19 for both inlets in the left-hand nacelle. As sideslip is increased to positive angles, evidence of nose gear wake ingestion is indicated initially in the inboard inlets as expected. Planar components maximized at a sideslip angle of approximately six degrees and then diminished at higher sideslip angles as the wake moved outboard of the nacelle. The impact of higher planar components in the outboard inlet is partially offset by lower spatial components.

Differences in flight test distortion characteristics between extended and retracted gear positions during operation at 5,000 feet, mach 0.35, are shown in Figure 20. With the gear up, the cowl lip is at 10 degrees, and with the gear down, the cowl lip is at 40 degrees. Angle of attack varies between 5.5 and 7 degrees, and engine airflow is maximum at 356 lb/sec. Extending the gear introduces a planar component with a peak-to-peak amplitude of 0.069. Circumferential distortion never exceeds eight percent, and the low-pressure defect appears in the upper cowl-side portion of the engine face. On the other hand, retracting the gear eliminates the planar component, and decreasing the cowl lip angle to 10 degrees increases circumferential distortion to approximately 11 percent. More radial distortion is evident, and the low pressure defect is located in the lower cowl-side quadrant. Operating the cowl lip at 40 degrees when the gear is down thus results in additional margin to accommodate potential ingestion of planar components.

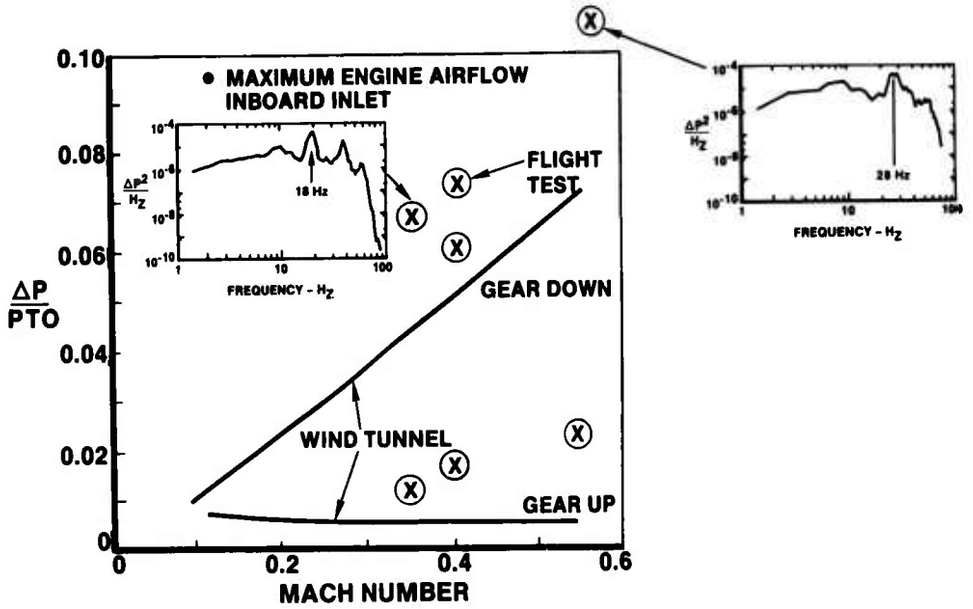

Figure 18. Effect of Gear Wake Ingestion on Planar Distortion

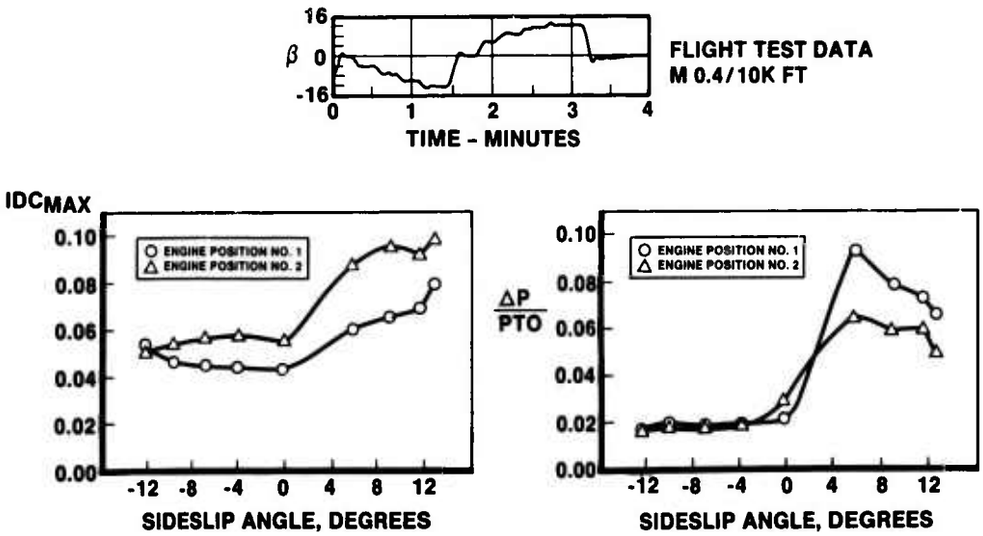

Figure 19. Nose Gear Wake Ingestion During Sideslip Operation

Wind tunnel and flight test distortion characteristics are compared in Figure 21. Test conditions were at mach 0.4, landing gear extended, with the aircraft (model) at 9 to 10 degrees sideslip and nominal angle of attack. Engine airflow was maximum at approximately 360 lb/sec. Differences in several distortion parameters are summarized in the table and are believed to be representative of the differences one should expect when comparing dynamic output of dynamic events.

Source	IDC	IDR	ΔP/PTO	f
Flight test	0.095	0.031	0.058	18
Wind tunnel	0.086	0.047	0.050	20 (scaled)

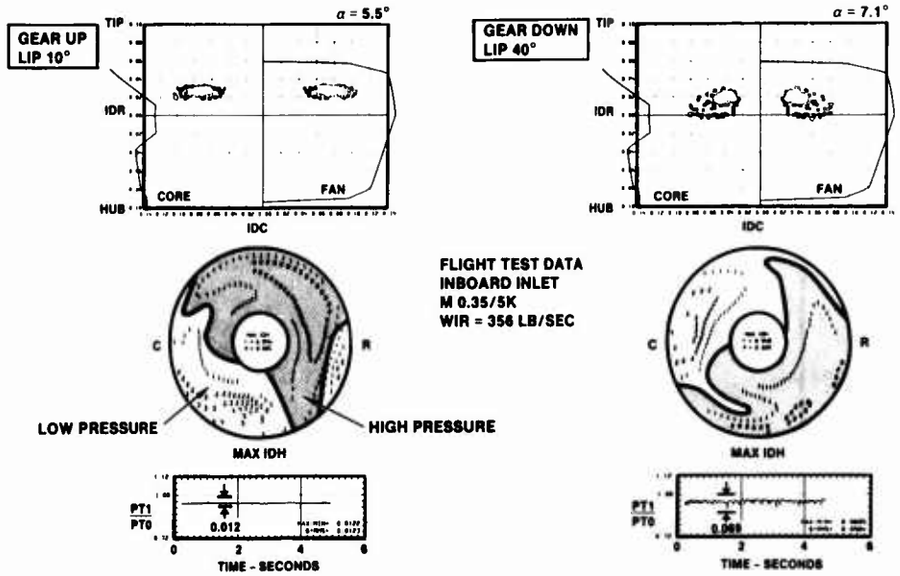

Figure 20. Effect of Gear Position on Inboard Inlet Distortion

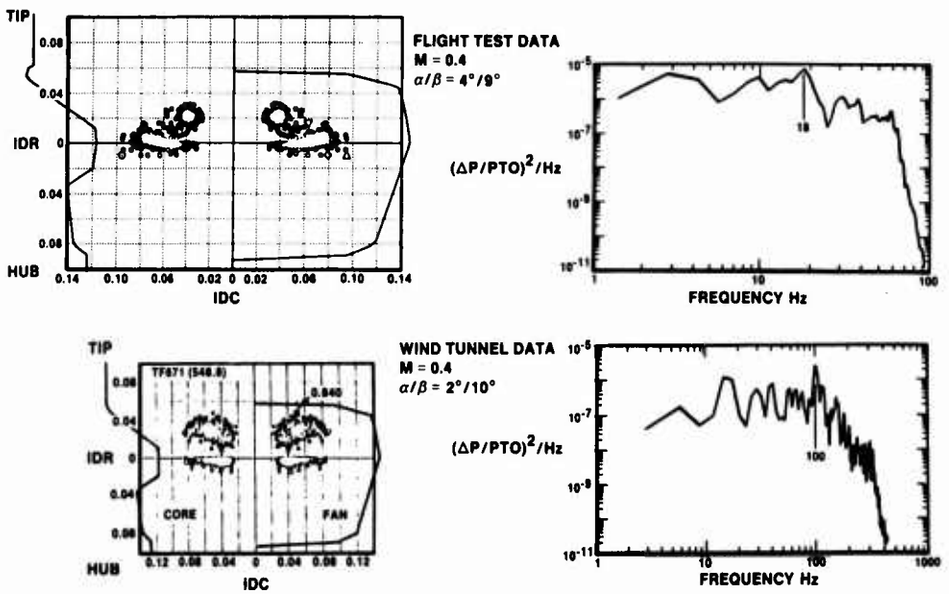

Figure 21. Wind Tunnel/Flight Test Comparison of Nose Gear Wake Effects

CONCLUDING REMARKS

Engine response to combinations of planar and spatial total-pressure distortion components is not well understood. Yet their consequences can be substantial, both in terms of engine stability and structural fatigue criteria. The most obvious solution is, of course, to eliminate the source of the disturbances. If this is not consistent with sound engineering practices, trades must be conducted to find cost-effective solutions.

Several sources of unsteady, one-dimensional pressure oscillations have been characterized with the B-1B program. Trends are summarized in Figure 22 and indicate that aircraft generated peak-to-peak amplitudes generally decrease as frequency increases. This is contrasted to estimated engine trends where one might expect more tolerance to amplitude at higher frequencies.

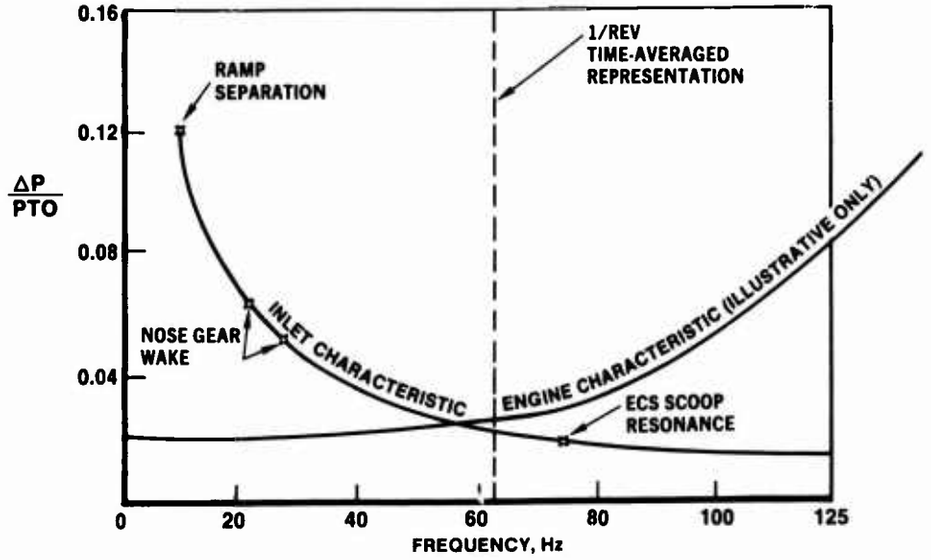

Figure 22. B-1B Planar Distortion Summary

Frequencies of planar components are generally configuration dependent. In cases where the source is duct resonance, good correlations exist between acoustic theory and test results. If wind tunnel models contain an acoustic reflection plane close to the simulated engine face, frequencies can be scaled accurately at constant Strouhal number, $fL/\sqrt{T}$. In the B-1B inlet development wind tunnel program, flow control vanes, located just aft of the aerodynamic interface plane, were operated choked over most conditions and provided this function.

In cases where the source is attributed to the ingestion of wakes or vortices shed by forward protuberances, frequencies are difficult to predict. Accurate simulation of the protuberance in the wind tunnel model is necessary to obtain reasonable correlations with flight test results. Peak-to-peak amplitudes measured with the flight test aircraft were generally higher than magnitudes measured with the 0.2-scale model. Amplitudes can be strong functions of freestream mach number.

Several design features were incorporated in the B-1B propulsion system as a result of planar distortion considerations. The inlet ramp was cut back to reduce flow separation along the lower ramp surface and significantly reduced planar amplitudes. An idle speed lockup control was incorporated to limit flight idle operation to airflows corresponding to 90 percent corrected core speeds. This function is currently controlled with a cockpit switch and is implemented during operation at high speeds and freestream dynamic pressures. Planar distortion components contributed to the decision to incorporate a three-position cowl lip design. This control assures that the inlet lip is in the most open position when the landing gear is extended. The flapper door separating the ECS precooler scoop located in the inlet from the ground blower circuit was redesigned to reduce discrete frequency components and relax structural fatigue criteria.

Many of these features are being evaluated in the ongoing flight test program, and no compatibility problems have been encountered. But the fact remains that flight test programs do not provide much insight on losses in stall pressure ratio, and the real measure of success in a compatibility program occurs only after thousands of hours of operation have been accumulated by the fleet. To really understand engine response to these disturbances, a well-constructed program to explore sensitivities to planar components operating in conjunction with various combinations of radial and circumferential spatial distortion components is needed. Frequency content of most of these disturbances falls well within the range of computational fluid dynamics technology. Combining this analytical approach with a systematic test program to measure effects on current turbofan engines sounds like a logical next step. Benefits on future aircraft designs and operational procedures could be substantial.

REFERENCES

1. SAE ARP 1420, "Gas Turbine Engine Inlet Flow Distortion Guidelines", March 1978

2. SAE AIR 1419, "Inlet Total-Pressure-Distortion Considerations for Gas Turbine Engines", May 1983

3. R. H. Johnson, NASA-CR-144864, "Comparison of Inlet Distortion from Flight and Wind Tunnel Tests", April 1978

4. Reynolds, G. G. and Steenken, W. G., AFAPL-TR-76-76, "Dynamic Digital Blade Row Compression Component Stability Model - Model Validation and Analysis of Planar Pressure Pulse Generator and Two-Stage Fan Test Data", August 1976

5. J. H. Wykes, et al, NASA-CR-144887, "Analyses and Test of the B-1 Aircraft Structural Mode Control System", January 1980